

# Unlocking Temporal Flexibility: Neural Speech Codec with Variable Frame Rate

Hanglei Zhang<sup>1</sup>, Yiwei Guo<sup>1</sup>, Zhihan Li<sup>1</sup>, Xiang Hao<sup>2</sup>, Xie Chen<sup>1</sup>, Kai Yu<sup>1</sup>

<sup>1</sup>MoE Key Lab of Artificial Intelligence, Jiangsu Key Lab of Language Computing, X-LANCE Lab, School of Computer Science, Shanghai Jiao Tong University, China

<sup>2</sup>Department of Data Science and Artificial Intelligence, The Hong Kong Polytechnic University, China

op.131@sjtu.edu.cn, kai.yu@sjtu.edu.cn

## Abstract

Most neural speech codecs achieve bitrate adjustment through intra-frame mechanisms, such as codebook dropout, at a Constant Frame Rate (CFR). However, speech segments inherently have time-varying information density (e.g., silent intervals versus voiced regions). This property makes CFR not optimal in terms of bitrate and token sequence length, hindering efficiency in real-time applications. In this work, we propose a Temporally Flexible Coding (TFC) technique, introducing variable frame rate (VFR) into neural speech codecs for the first time. TFC enables seamlessly tunable average frame rates and dynamically allocates frame rates based on temporal entropy. Experimental results show that a codec with TFC achieves optimal reconstruction quality with high flexibility, and maintains competitive performance even at lower frame rates. Our approach is promising for the integration with other efforts to develop low-frame-rate neural speech codecs for more efficient downstream tasks.

**Index Terms:** neural speech codec, speech coding, variable frame rate, information density

## 1. Introduction

Recent audio/speech codecs have integrated neural networks to achieve high-fidelity audio reconstruction [1, 2, 3]. These models are typically trained end-to-end and consist of three main components: an encoder that compresses the input signal into compact representations, a quantization module that discretizes these representations, and a decoder that reconstructs the audio from the quantized vectors. Owing to their success, discrete token-based generative modeling has been successfully extended to the speech domain, leading to speech generation models such as AudioLM [4] and VALL-E [5].

However, existing neural speech codecs generate token sequences at a high temporal rate—up to 75 frames per second for systems such as EnCodec [2]—whereas text tokenization using BPE [6] typically yields only 3–5 tokens per second. This significant discrepancy in token lengths results in inefficient autoregressive prediction, causing performance degradation and increased latency in real-time applications [7]. In addition to efforts aimed at improving the efficiency of downstream speech generation models themselves [8, 9, 10], several recent studies have begun to explore low-frame-rate neural audio codecs to fundamentally address this challenge [11, 12, 13, 14, 15].

Despite these efforts, we also observe that most neural speech codecs operate as Constant Bitrate (CBR) systems, which could lead to redundant coding, especially for segments like silence where a lower coding rate would suffice compared to highly dynamic areas. This temporal redundancy undermines

the goal of minimizing both overall bitrate consumption and sequence length. While prior work [16] has preliminarily incorporated a Variable Bitrate (VBR) strategy based on information density, it still belongs to the Constant Frame Rate (CFR) framework and does not reduce the overall sequence length. To the best of our knowledge, a Variable Frame Rate (VFR) strategy has not yet been introduced to the neural speech codec field.

Accordingly, we propose **Temporally Flexible Coding (TFC)** for neural speech codecs with two primary objectives: (1) to shorten the overall sequence lengths produced at a given total bitrate, and (2) to enable dynamic frame rate allocation that achieves better temporal compactness and flexibility.

TFC introduces VFR coding to neural speech codecs by dynamically adjusting output codes’ receptive fields along the temporal axis. Inspired by techniques from variable-rate image compression [17] and early analyses of speech information entropy in the VFR context [18], we leverage a non-parametric entropy calculation technique on speech segments to gauge their information density for dynamic frame rate allocation. High-entropy regions, which indicate information-rich content, are allocated higher frame rates, while low-entropy regions, such as silence, are assigned lower frame rates. In summary, TFC enables **a single model to support a user-specified average frame rate ranging from 18.75 Hz to 75 Hz** (following DAC [3] backbone for 24kHz audio), and **ensures a reasonable distribution of time-varying frame rates under a specific total bitrate**.

Overall, TFC achieves both flexible frame rate control and interpretable granularity allocation within a unified framework. It presents a novel contribution to speech coding by introducing VFR to neural speech codecs for the first time. Furthermore, the design of TFC can be orthogonally integrated with other techniques aimed at reducing sequence length and overall bitrate, demonstrating broad and promising application prospects.

## 2. Background

This section situates our work within the broader context of development in feature compression, providing a comprehensive discussion of terms CBR, VBR, CFR, and VFR, as well as the necessary notations for further understanding.

### 2.1. Constant versus Variable Bitrate in Neural Codecs

The concepts of **Constant Bitrate (CBR)** and **Variable Bitrate (VBR)** in audio/speech codecs are defined in the temporal domain. In CBR, the codec maintains a fixed number of bits per unit time, whereas VBR enables dynamically adjusting the temporal bit allocation based on the complexity of the signal.

Formally, let  $\mathbf{z}_e = f_\theta(\mathbf{x}) \in \mathbb{R}^{D \times T}$  denote the continuous latent representations of audio  $\mathbf{x}$ , encoded by  $f_\theta(\cdot)$ , where  $T$

Kai Yu is the corresponding author.

represents the number of downsampled temporal frames, and  $D$  is the dimensionality of the latent vectors. At a specific frame  $t$ , the latent vector  $\mathbf{z}_e[t]$  is quantized to obtain  $\mathbf{z}_q[t]$ . In an RVQ-based codec with  $N_q$  quantizers,  $\mathbf{z}_q[t]$  is computed as  $\mathbf{z}_q[t] = \sum_{i=1}^{N_q} Q_i(\mathbf{r}_i[t])$  where  $Q_i(\cdot)$  is the  $i$ -th quantizer, and the residual vector  $\mathbf{r}_i[t]$  is defined recursively as:

$$\mathbf{r}_i[t] = \begin{cases} \mathbf{z}_e[t] & i = 1, \\ \mathbf{r}_{i-1}[t] - Q_{i-1}(\mathbf{r}_{i-1}[t]) & 2 \leq i \leq N_q. \end{cases} \quad (1)$$

The reconstructed audio is then obtained as  $\hat{\mathbf{x}} = g_\psi(\mathbf{z}_q)$  using the decoder  $g_\psi(\cdot)$ .

The quantizer dropout strategy introduced in [1] allows a single RVQ-based codec to operate at multiple target bitrates. Specifically, by randomly sampling  $n_q \sim \{1, \dots, N_q\}$  and using only the first  $n_q$  quantizers for different samples during training, the user can flexibly select  $n_q$  at inference time, where a lower  $n_q$  results in lower reconstruction quality but reduced bitrate usage. However, this trick alone does not change the fact that RVQ-based codecs allocate the same number of codebooks across all temporal frames under a fixed frame rate, making them effectively CBR. The needs in generative speech modeling have spurred new concepts for neural codecs, such as single-codebook [19, 14, 20], multi-resolutions [21, 22], and low-frame-rate or low-bitrate codecs [11, 13, 15, 23]. Although these designs empower downstream real-time dialogue applications [12, 24], they remain within the CBR paradigm.

Recently, VRVQ [16] introduced the VBR strategy into RVQ-based neural audio codecs. It assigns a time-varying  $n_q$  to different downsampled frames based on a neural-predicted importance map at inference time. The design of VRVQ aligns well with efforts to reduce the overall bitrate consumption, but it does not reduce the number of frames.

## 2.2. Variable Frame Rate Compression

Although achieving VBR coding, VRVQ still operates at a **Constant Frame Rate (CFR)**, meaning that each encoded frame represents a fixed temporal window of the signal. Low frame rates are particularly important for autoregressive modeling, motivating the need to clarify the broader concept of VBR and to discuss **Variable Frame Rate (VFR)** codecs.

In the context of audio compression, VBR does not necessarily imply VFR, especially in RVQ-based codecs where each frame can contain multiple quantizers. Here, we define VFR as a coding strategy that **allows each encoded frame to adaptively cover different temporal spans**. It indicates that the model can effectively adjust the downsampling rate based on information density. For example, a code in VFR setting can cover a longer time span during silent periods and a shorter span during rapidly-changing phoneme transitions.

The VFR concept has been implemented in semantic tokens derived from speech self-supervised learning models [25], which are primarily designed for discriminative tasks such as ASR. For these tokens, preserving fine-grained acoustic details is less critical, and VFR compression can be achieved through distillation from pretrained models or unit discovery techniques [26, 27]. However, acoustic tokens from neural codecs inherently encode more detailed information; hence, assigning different coding granularities becomes less straightforward due to the absence of explicit supervisory labels that are available for semantic tokens. This necessitates the development of effective heuristic strategies for variable frame rate allocation. Inspired from variable rate coding methods in im-

age compression[28, 17] that adjust spatial resolution based on content complexity, we introduce the VFR strategy to speech codecs to adaptively manage the temporal resolution.

## 3. Temporally Flexible Coding

In this section, we will describe our proposed TFC strategy. TFC is a plug-and-play module that can be integrated to various codec backbones like DAC [3], without introducing additional losses for optimization.

### 3.1. Measuring Information Density by Temporal Entropy

To measure the information density of a speech segment for granularity allocation in VFR coding, we choose a non-parametric entropy-based approach. Note that an alternative is to use a neural router for granularity allocation [28], but this introduces the risk of instability in gradient estimation, and is reported to perform worse than entropy-based methods in [28]’s implementation. Thus we make adaptations upon the algorithm originally designed for spatial entropy [29, 17] to fit the temporal information in speech signals.

Assume  $\mathcal{T}$  is a temporal segment, and  $\mathbf{x}[t] \in [-1, 1]$  represents the amplitude value of normalized speech signal  $\mathbf{x}$  at  $t \in \mathcal{T}$ . We define  $N$  uniformly spaced bins  $\{u_1, u_2, \dots, u_N\}$  spanning  $[-1, 1]$  as  $u_i = -1 + \frac{2i}{N-1}$  for  $i = 0, 1, \dots, N-1$ . To estimate the probability density of  $\mathbf{x}[t]$  across these bins, we compute its Gaussian affinity  $p_{t,i}$  to each bin  $u_i$ :

$$p_{t,i} = \exp\left(-\frac{(\mathbf{x}[t] - u_i)^2}{2\sigma^2}\right), \quad (2)$$

where  $\sigma$  controls distribution sharpness. This models the likelihood of  $\mathbf{x}[t]$  “diffusing” to bin  $u_i$ .

For a segment  $\mathcal{T}$ , we average affinities across all  $|\mathcal{T}|$  samples in  $\mathcal{T}$  and normalize them to form a probability distribution:

$$p_{\mathcal{T},i} = \frac{1}{|\mathcal{T}|} \sum_{t \in \mathcal{T}} p_{t,i}, \quad \overline{p_{\mathcal{T},i}} = \frac{p_{\mathcal{T},i}}{\sum_{j=0}^{N-1} p_{\mathcal{T},j} + \epsilon}, \quad (3)$$

where  $\epsilon$  ensures numerical stability. The temporal entropy of  $\mathcal{T}$  is computed with Shannon Entropy:

$$H(\mathcal{T}) = - \sum_{i=0}^{N-1} \overline{p_{\mathcal{T},i}} \log \overline{p_{\mathcal{T},i}} \quad (4)$$

The computed entropy values, indicating the information densities in specific temporal windows  $\mathcal{T}$ , are used for dynamically allocating frame rates described in next section.

### 3.2. Encoder with Variable Frame Rate Allocation

Let the codec encoder backbone output representation sequence  $\mathbf{z}_f$  with a receptive field  $w_f = W$  sampling points and stride  $s$ . We denote its frame rate as  $F$ , corresponding to **fine-resolution representations**  $\mathbf{z}_f$ . We then generate two additional subsampled representation sequences of  $\mathbf{z}_f$  by CNN blocks:

- **Medium-resolution representations**  $\mathbf{z}_m$ , downsampled from  $\mathbf{z}_f$  with frame rate  $F/2$ , stride  $2s$  and each frame’s receptive field  $w_m = W + s$  sampling points.
- **Coarse-resolution representation**  $\mathbf{z}_c$ , downsampled from  $\mathbf{z}_m$  with frame rate  $F/4$ , stride  $4s$  and each frame’s receptive field  $w_c = W + 3s$  sampling points.

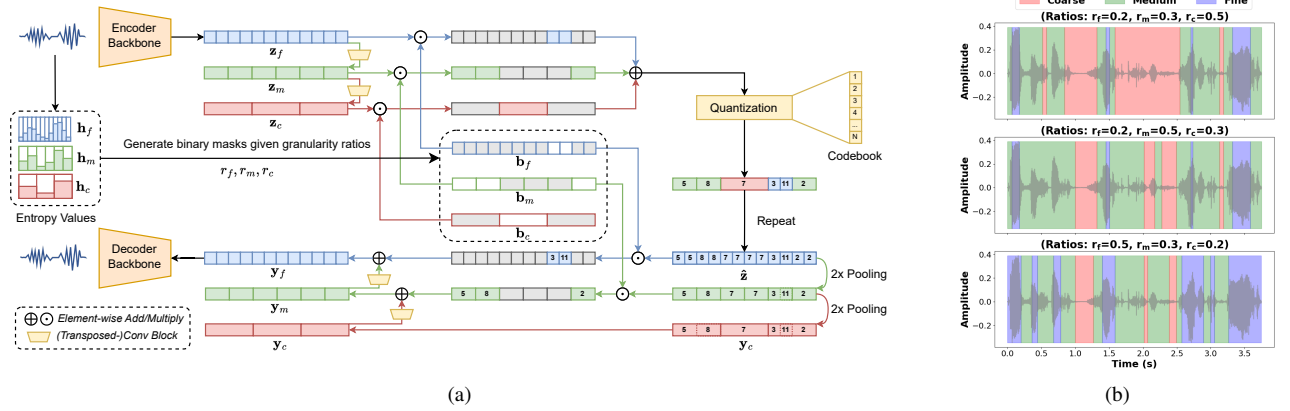


Figure 1: (a) Proposed framework of Temporally Flexible Coding. (b) VFR allocation examples under different granularity ratios.

For each resolution, we compute entropy values based on Section 3.1, where the size of  $\mathcal{T}$  is set to the corresponding receptive field, and temporal segments are slid by the corresponding stride. Denote  $\mathbf{h}_f, \mathbf{h}_m, \mathbf{h}_c$  as the scalar entropy sequences for fine, medium and coarse resolution, respectively, each conforming to the frame rate of  $\mathbf{z}_f, \mathbf{z}_m, \mathbf{z}_c$ .

Then, we combine the three resolutions together to form a VFR representation. Given user-defined non-negative scalar granularity ratios  $r_f, r_m, r_c$  with  $r_f + r_m + r_c = 1$ , we firstly generate binary sequential granularity masks  $\mathbf{b}_c, \mathbf{b}_m, \mathbf{b}_f$  by:

$$\begin{aligned} \mathbf{b}_c &= \mathbb{1}(\mathbf{h}_c \leq \text{Quantile}_{r_c}(\mathbf{h}_c)) \\ \mathbf{h}'_m &= \mathbf{h}_m \odot (1 - (\mathbf{b}_c) \uparrow_2) \\ \mathbf{b}_m &= \mathbb{1}(\mathbf{h}'_m \leq \text{Quantile}_{\frac{r_m}{1-r_c}}(\mathbf{h}'_m)) \\ \mathbf{b}_f &= 1 - (\mathbf{b}_m) \uparrow_2 - (\mathbf{b}_c) \uparrow_4 \end{aligned} \quad (5)$$

where  $\mathbb{1}(\cdot)$  is the indicator function, and  $\text{Quantile}_q(\mathbf{h})$  represents the  $q$ -quantile of  $\mathbf{h}$  within each utterance.  $(\cdot) \uparrow_k$  denotes repeating operations by factor  $k$ .  $\mathbf{h}'_m$  represents the remaining part in  $\mathbf{h}_m$  that is not masked by  $\mathbf{b}_c$ . The binary masks  $\mathbf{b}$  have the same frame rate as that of the corresponding  $\mathbf{h}$  and  $\mathbf{z}$  for each resolution. As a result, a 1-second speech segment will yield  $Fr_c/4$  coarse-grained frames,  $Fr_m/2$  medium-grained frames and  $Fr_f$  fine-grained frames before quantization, whose temporal spans follow a  $r_c:r_m:r_f$  ratio.

Subsequently, for each resolution, the continuous representations are quantized to produce  $\hat{\mathbf{z}}_f, \hat{\mathbf{z}}_m, \hat{\mathbf{z}}_c$ , using the RVQ process described in (1). To fuse these representations into a unified feature sequence  $\hat{\mathbf{z}}$  that aligns with the finest temporal resolution, we repeat the medium and coarse quantized vectors, and integrate them via element-wise multiplication  $\odot$  with their corresponding masks:

$$\hat{\mathbf{z}} = (\hat{\mathbf{z}}_f \odot \mathbf{b}_f) + (\hat{\mathbf{z}}_m \odot \mathbf{b}_m) \uparrow_2 + (\hat{\mathbf{z}}_c \odot \mathbf{b}_c) \uparrow_4 \quad (6)$$

Generally, this hierarchical design allows multiple temporal resolutions to be represented with one frame of codebook indexes, reducing the encoded bitrate for low-entropy area by a smaller frame rate. Figure 1b exemplifies this allocation strategy, where we can find clearly that coarse frames are mostly allocated to silent segments, and granularity ratios can be conveniently adjusted for different frame rates.

### 3.3. Decoder with Conditional Hierarchical Design

Inspired by [17], we adopt a conditional hierarchical design in decoder to progressively refine the fused latent represen-

tations after quantization by gradually integrating information from coarser to finer scales. Given the binary granularity masks  $\{\mathbf{b}_f, \mathbf{b}_m, \mathbf{b}_c\}$ , the decoder processes the latent representation  $\hat{\mathbf{z}}$  as follows:

- The coarse representation  $\mathbf{y}_c$  is derived by downsampling  $\hat{\mathbf{z}}$  via average pooling:  $\mathbf{y}_c = (\hat{\mathbf{z}}) \downarrow_4$ .
- The medium representation  $\mathbf{y}_m$  is conditioned on  $\mathbf{y}_c$ , combined with original quantized medium-resolution latent features. Specifically, we use a transposed CNN block to up-sample  $\mathbf{y}_c$  by a factor of 2, and add the upsampled sequence with  $(\hat{\mathbf{z}}) \downarrow_2 \odot \mathbf{b}_m$ .
- The finest representation  $\mathbf{y}_f$  integrates both  $\mathbf{y}_m$  and  $\mathbf{y}_c$ , fused with original quantized fine-resolution latent  $\hat{\mathbf{z}} \odot \mathbf{b}_f$ . Similarly, this is also achieved via upsampling  $\mathbf{y}_m$  using a transposed CNN, before adding with  $\hat{\mathbf{z}} \odot \mathbf{b}_f$ .

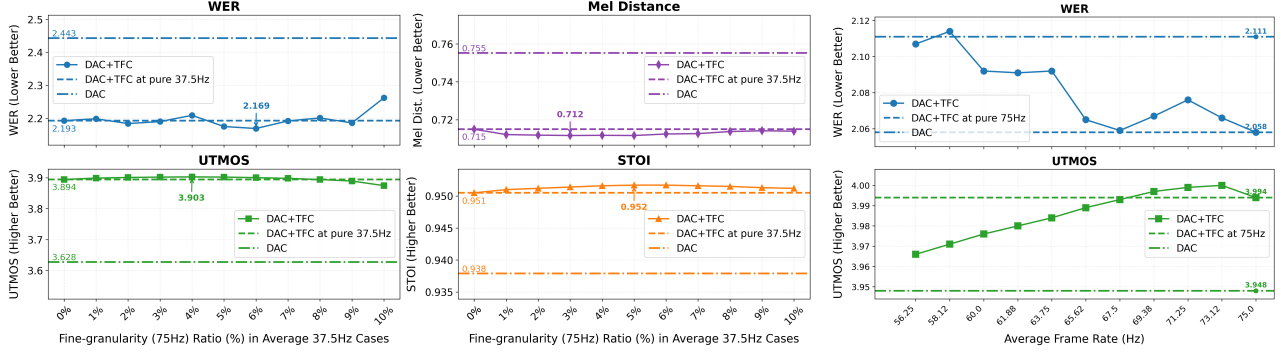
Overall, each layer refines its predecessor's output by aggregating reconstructed features with earliest quantized features, avoiding potential error propagation when solely relying on former reconstructed results. Finally,  $\mathbf{y}_c$  with original frame rate  $F$  is passed to codec decoder backbone to recover waveform.

## 4. Experiments

### 4.1. Architecture and Setup

We implement TFC upon the DAC [3] backbone, which achieves high-fidelity reconstruction performance among various existing codecs [30]. We use its official configuration for 24kHz audio that produces RVQ codes at 75Hz frame rate. Hence in our DAC+TFC framework, the finest granularity is  $F = 75\text{Hz}$ . Our hierarchical design described in Section 3.2 performs 2 times  $2\times$  downsampling with CNN blocks to obtain medium and coarse representations, and upsamplings as in Section 3.3 with transposed CNN blocks reversely. The encoded representations are quantized using 8-dimensional RVQ with 1024 (10 bits) entries and maximum codebook number  $N_q = 32$ . As this results in a large bitrate (24kbps) that is not practical for downstream generative applications, we take advantage of codebook dropout to use at most 8 codebooks (6kbps) in inference stage.

Both the DAC baseline and the proposed DAC+TFC model are trained on LibriTTS [31] with 960 hours of speech data. To ensure sufficient training across different temporal resolutions, batch inputs for DAC+TFC are heuristically allocated with frame rate ratios  $r_f = 0.4, r_m = 0.3, r_c = 0.3$ . Each model is trained with a batch size of 20 with 1-second clipped



(a) Results for inferences under average 3kbps/37.5Hz. (b) Results for VFR (<75Hz) and CFR (75Hz).  
Figure 2: DAC+TFC (solid lines) is evaluated in VFR mode compared to CFR performances (dashed lines).

segments for 1000k iterations.

Reconstruction quality is measured via Mel and STFT distances (configurations following [3]), with the latter better capturing high-frequency fidelity. Additionally, perceptual quality is assessed using UTMOS [32], a MOS prediction system that correlates strongly with human ratings, as well as STOI (Short-time Objective Intelligibility) and WER metrics<sup>1</sup>, ensuring a comprehensive evaluation.

#### 4.2. Result A: CFR performances across different bitrates

DAC+TFC supports frame rate selection from 18.75Hz to 75Hz by adjusting the granularity ratios in inference. It can be viewed as an alternative method for bitrate control along with codebook dropout. For the DAC baseline, we can select different bitrates by specifying the number of codebooks in inference. Thus we can conduct fair comparisons between DAC and the proposed DAC+TFC under the same bitrates. For example, if we use DAC with 4 codebooks to inference, it has a bitrate of 3kbps; then, we compare it with DAC+TFC at 37.5Hz with 8 codebooks that also has a bitrate of 3kbps.

Table 1: Reconstruction performances of DAC and proposed DAC+TFC in a CFR manner with different bitrates

Bitrate (kbps)	Model	Frame Rate (Hz)	$N_q$	Mel Dist. ↓	STFT Dist. ↓	UTMOS ↑	STOI ↑	WER ↓
6	DAC	75	8	<b>0.594</b>	1.456	3.948	0.967	4.125
	DAC+TFC	75	8	0.601	<b>1.451</b>	<b>3.994</b>	<b>0.970</b>	<b>2.845</b>
3	DAC	75	4	0.755	1.617	3.628	0.938	2.443
	DAC+TFC	37.5	8	<b>0.715</b>	<b>1.565</b>	<b>3.895</b>	<b>0.951</b>	<b>2.193</b>
1.5	DAC	75	2	0.930	1.792	2.869	0.892	2.110
	DAC+TFC	18.75	8	<b>0.864</b>	<b>1.725</b>	<b>2.995</b>	<b>0.902</b>	<b>2.058</b>

The corresponding results are shown in Table 1. Notably, DAC+TFC achieves better performance than DAC across most metrics, especially in terms of WER. These results show that TFC effectively controls bitrate, preserves audio quality, and meets the initial goal of reducing sequence length. This can be beneficial for downstream generative models [4, 5, 33, 12] since reducing frame count will greatly speed up the generation process, while increased number of codebooks has a negligible impact on generation speed.

<sup>1</sup>Computed with NeMo ASR: [https://huggingface.co/nvidia/stt\\_en\\_fastconformer\\_transducer\\_large](https://huggingface.co/nvidia/stt_en_fastconformer_transducer_large)

#### 4.3. Result B: VFR versus CFR performances

In Section 4.2, while showing basic temporal flexibility, TFC still operates in a CFR way as the frame rates are directly obtained by purely assigning one granularity. In this section, we evaluate TFC under truly VFR conditions, i.e. where at least two granularities are combined during inference.

First, we compare VFR and CFR cases at the same average frame rate. We adopt an average 3kbps bitrate & 37.5Hz frame rate setting because it permits mixing components at 18.75Hz and 75Hz (by 2:1 ratios) via TFC to yield VFR results (e.g. by setting  $r_f, r_m, r_c$  to 0.2, 0.7, 0.1, respectively). Figure 2a obviously shows the consistent improvement brought by TFC when mixing other frame rates compared to pure 37.5Hz (0% 75Hz granularity) and 3kbps DAC in terms of Mel Distance, UTMOS, and STOI metrics. Moreover, the lowest WER is achieved with 6% 75Hz component. Overall, these results underscore TFC’s flexibility in customizing frame rates and its superior performance benefited from VFR coding.

To further explore the potential of TFC, we compare its VFR results at lower frame rates with 75Hz CFR settings. Since lower bitrates from same architecture inevitably degrade reconstruction quality, we focus on UTMOS and WER to assess perceptual quality. The results (all with  $N_q = 8$ ) include the 75Hz DAC baseline, as well as DAC+TFC configurations, with frame rate ratios  $r_c:r_m:r_f$  smoothly varying from 0:0:100% (purely 75Hz frame rate) to 0:50%:50% (an average of 56.25Hz frame rate). As shown in Figure 2b, aside from one outlier in WER, the DAC+TFC configurations consistently outperform the 75Hz DAC baseline. Notably, some lower frame rate settings even achieve higher UTMOS scores than the 75Hz DAC+TFC configuration, indicating the significant potential of VFR design to compress speeches more compactly.

## 5. Conclusion

We present Temporally Flexible Coding (TFC), a method that introduces Variable Frame Rate (VFR) into neural speech codecs to dynamically adjust temporal resolution based on information density. TFC effectively balances bitrate and audio quality while reducing sequence length. Due to resource constraints, our implementation is limited to one codec backbone; future work will extend to architecture ablations, as well as evaluations on downstream generation. We believe that VFR paradigm holds significant potential for broader applications in neural speech coding and future generative speech models.

## 6. Acknowledgements

This work was supported by the China NSFC Project (No. 92370206), the Shanghai Municipal Science and Technology Major Project (2021SHZDZX0102) and the Key Research and Development Program of Jiangsu Province, China (No.BE2022059).

## 7. References

- [1] N. Zeghidour, A. Luebs, A. Omran *et al.*, “SoundStream: An End-to-End Neural Audio Codec,” *IEEE/ACM Trans. ASLP*, vol. 30, pp. 495–507, 2021.
- [2] A. Défossez, J. Copet, G. Synnaeve *et al.*, “High Fidelity Neural Audio Compression,” *Transactions on Machine Learning Research*, 2023.
- [3] R. Kumar, P. Seetharaman, A. Luebs *et al.*, “High-Fidelity Audio Compression with Improved RVQGAN,” *Proc. NeurIPS*, vol. 36, 2024.
- [4] Z. Borsos, R. Mariner, D. Vincent *et al.*, “AudioLM: A Language Modeling Approach to Audio Generation,” *IEEE/ACM Trans. ASLP*, vol. 31, pp. 2523–2533, 2023.
- [5] S. Chen, C. Wang, Y. Wu, Z. Zhang, L. Zhou, S. Liu, Z. Chen, Y. Liu, H. Wang, J. Li, L. He, S. Zhao, and F. Wei, “Neural Codec Language Models are Zero-Shot Text to Speech Synthesizers,” *IEEE/ACM Trans. ASLP*, pp. 1–15, 2025.
- [6] R. Sennrich, B. Haddow, and A. Birch, “Neural machine translation of rare words with subword units,” in *Proceedings of the 54th Annual Meeting of the Association for Computational Linguistics (Volume 1: Long Papers)*. Association for Computational Linguistics, Aug. 2016, pp. 1715–1725.
- [7] H. Wang, H. Wang, Y. Guo *et al.*, “Why Do Speech Language Models Fail to Generate Semantically Coherent Outputs? A Modality Evolving Perspective,” *arXiv preprint arXiv:2412.17048*, 2024.
- [8] S. Chen, S. Liu, L. Zhou, Y. Liu, X. Tan, J. Li, S. Zhao, Y. Qian, and F. Wei, “VALL-E 2: Neural codec language models are human parity zero-shot text to speech synthesizers,” *arXiv preprint arXiv:2406.05370*, 2024.
- [9] Y. Song, Z. Chen, X. Wang, Z. Ma, G. Yang, and X. Chen, “TacoLM: Gated attention equipped codec language model are efficient zero-shot text to speech synthesizers,” in *Proc. ISCA Interspeech*, 2024, pp. 4433–4437.
- [10] B. Li, H. Wang, S. Zhang, Y. Guo, and K. Yu, “Fast and high-quality auto-regressive speech synthesis via speculative decoding,” in *Proc. IEEE ICASSP*, 2025.
- [11] E. Casanova, R. Langman, P. Neekhara *et al.*, “Low Frame-Rate Speech Codec: a Codec Designed for Fast High-quality Speech LLM Training and Inference,” *arXiv preprint arXiv:2409.12117*, 2024.
- [12] A. Défossez, L. Mazaré, M. Orsini *et al.*, “Moshi: A Speech-Text Foundation Model for Real-Time Dialogue,” *arXiv preprint arXiv:2410.00037*, 2024.
- [13] H. Liu, X. Xu, Y. Yuan, M. Wu, W. Wang, and M. D. Plumbley, “SemantiCodec: An ultra low bitrate semantic audio codec for general sound,” *IEEE Journal of Selected Topics in Signal Processing*, vol. 18, no. 8, pp. 1448–1461, 2024.
- [14] S. Ji, Z. Jiang, W. Wang *et al.*, “WavTokenizer: an Efficient Acoustic Discrete Codec Tokenizer for Audio Language Modeling,” in *Proc. ICLR*, 2025.
- [15] J. D. Parker, A. Smirnov, J. Pons, C. Carr, Z. Zukowski, Z. Evans, and X. Liu, “Scaling transformers for low-bitrate high-quality speech coding,” in *Proc. ICLR*, 2025.
- [16] Y. Chae, W. Choi, Y. Takida *et al.*, “Variable Bitrate Residual Vector Quantization for Audio Coding,” *arXiv preprint arXiv:2410.06016*, 2024.
- [17] A. Li, F. Li, Y. Liu, R. Cong, Y. Zhao, and H. Bai, “Once-for-all: Controllable generative image compression with dynamic granularity adaption,” in *Proc. ICLR*, 2025.
- [18] H. You, Q. Zhu, and A. Alwan, “Entropy-based variable frame rate analysis of speech signals and its application to ASR,” in *Proc. IEEE ICASSP*, vol. 1, 2004, pp. I–549.
- [19] H. Li, L. Xue, H. Guo *et al.*, “Single-Codec: Single-Codebook Speech Codec towards High-Performance Speech Generation,” in *Proc. ISCA Interspeech*, 2024, pp. 3390–3394.
- [20] Y. Guo, Z. Li, C. Du *et al.*, “LSCoDec: Low-Bitrate and Speaker-Decoupled Discrete Speech Codec,” *arXiv preprint arXiv:2410.15764*, 2024.
- [21] H. Siuzdak, F. Grötschla, and L. A. Lanzendörfer, “SNAC: Multi-Scale Neural Audio Codec,” *arXiv preprint arXiv:2410.14411*, 2024.
- [22] H. Guo, F. Xie, D. Yang, X. Wu, and H. Meng, “Speaking from coarse to fine: Improving neural codec language model via multi-scale speech coding and generation,” *arXiv preprint arXiv:2409.11630*, 2024.
- [23] H. Wu, N. Kanda, S. E. Eskimez, and J. Li, “TS3-Codec: Transformer-based simple streaming single codec,” *arXiv preprint arXiv:2411.18803*, 2024.
- [24] Z. Xie and C. Wu, “Mini-Omni: Language Models Can Hear, Talk While Thinking in Streaming,” *arXiv preprint arXiv:2408.16725*, 2024.
- [25] A. Mohamed, H.-y. Lee, L. Borgholt, J. D. Havtorn, J. Edin, C. Igel, K. Kirchhoff, S.-W. Li, K. Livescu, L. Maaløe *et al.*, “Self-supervised speech representation learning: A review,” *IEEE Journal of Selected Topics in Signal Processing*, vol. 16, no. 6, pp. 1179–1210, 2022.
- [26] C. J. Cho, N. Lee, A. Gupta *et al.*, “Sylber: Syllabic Embedding Representation of Speech from Raw Audio,” in *Proc. ICLR*, 2025.
- [27] A. Baade, P. Peng, and D. Harwath, “SyllableLM: Learning Coarse Semantic Units for Speech Language Models,” in *Proc. ICLR*, 2025.
- [28] M. Huang, Z. Mao, Z. Chen, and Y. Zhang, “Towards accurate image coding: Improved autoregressive image generation with dynamic vector quantization,” in *Proc. IEEE/CVF CVPR*, 2023, pp. 22 596–22 605.
- [29] T. Celik, “Spatial entropy-based global and local image contrast enhancement,” *IEEE Transactions on Image Processing*, vol. 23, no. 12, pp. 5298–5308, 2014.
- [30] H. Wu, H.-L. Chung, Y.-C. Lin, Y.-K. Wu, X. Chen, Y.-C. Pai, H.-H. Wang, K.-W. Chang, A. Liu, and H.-y. Lee, “Codec-SUPERB: An in-depth analysis of sound codec models,” in *Findings of the Association for Computational Linguistics: ACL 2024*. Association for Computational Linguistics, Aug. 2024, pp. 10 330–10 348.
- [31] H. Zen, V. Dang, R. Clark, Y. Zhang, R. J. Weiss, Y. Jia, Z. Chen, and Y. Wu, “LibriTTS: A corpus derived from librispeech for text-to-speech,” in *Proc. ISCA Interspeech*, 2019, pp. 1526–1530.
- [32] T. Saeki, D. Xin, W. Nakata, T. Koriyama, S. Takamichi, and H. Saruwatari, “UTMOS: UTokyo-SaruLab System for Voice-MOS Challenge 2022,” in *Proc. ISCA Interspeech*, 2022, pp. 4521–4525.
- [33] P. Peng, P.-Y. Huang, S.-W. Li, A. Mohamed, and D. Harwath, “VoiceCraft: Zero-shot speech editing and text-to-speech in the wild,” in *Proceedings of the 62nd Annual Meeting of the Association for Computational Linguistics (Volume 1: Long Papers)*. Association for Computational Linguistics, Aug. 2024, pp. 12 442–12 462.